Numerical modelling of squeezing behaviour in tunnels

Giovanni Barla*, Stefania Borgna*

Summary

The paper describes a numerical modelling procedure which has been recently implemented in the Finite Difference code FLAC, with the main purpose to simulate the squeezing behaviour in tunnels. A stress-strain law is applied which considers three different stages of behaviour: the elastic stage, up to the onset of time dependent deformations; the hardening stage, which is intended to represent the terminal locus of long-term creep deformations; the softening stage. The results of a validation exercise for typical stress-strain laws obtained in triaxial compression tests and for the stress-strain distribution around a deep circular tunnel are briefly discussed.

1. Introduction

In order to analyse the behaviour of a tunnel in squeezing conditions, under the assumption of equivalent continuum, constitutive relationships need to be formulated to represent the most important factors influencing squeezing:

1. the onset of yielding within the rock mass, as determined by the shear strength parameters relative to the induced stress;
2. the time dependent behaviour.

The most appropriate constitutive relationships are of either the elasto-plastic or elasto-visco-plastic type. However, the use of such relationships is difficult if not impossible, in view of rock mass characterization (squeezing is associated with poor rock masses, with reduced quality indices such as RMR and Q) and assessment of deformability and strength parameters; also, the evaluation of viscous properties as needed in order to quantify the rock mass behaviour is quite problematic.

In the present paper a phenomenological model will be presented, which is intended to simulate the squeezing behaviour in tunnels. The formulation of such a model is based upon considerations derived from typical results of laboratory testing with a stiff testing machine and under constant loading [LADANYI, 1993]. It consists of simulating the observed stress-strain behaviour, without accounting directly for time-dependence, however adapting in a suitable manner the strength parameters of the Mohr-Coulomb criterion which is adopted.

* Department of Structural and Geotechnical Engineering – Politecnico di Torino.

2. Experimental evidence

As shown in figure 1 [LADANYI, 1993], the locus of a creep test in the $(\sigma_1\text{-}p)$-ε stress-strain plot is a horizontal line, intersecting the $(\sigma_1\text{-}p)$ axis for a stress value which is sustained during the test. For stress values below the threshold value σ_T, there is no time-dependent behaviour.

For stress values above σ_T and below σ_U, e.g. σ_E, creep is attenuating and stops at a finite strain ε_F even if loading is maintained constant for a significant time duration; it is therefore possible to attain a condition where the strain will be greater than the value holding true when no creep occurs (ε_E) of the amount $(\varepsilon_F\text{-}\varepsilon_E)$.

If a number of creep tests are performed, each one for a different value of the applied stress, the results obtained plot on the $(\sigma_1\text{-}p)$-ε plane by giving the terminal locus of long term creep tests (TU), without exhibiting any tertiary creep leading to creep failure. This type of behaviour will occur for a stress value greater than σ_U, resulting in the long

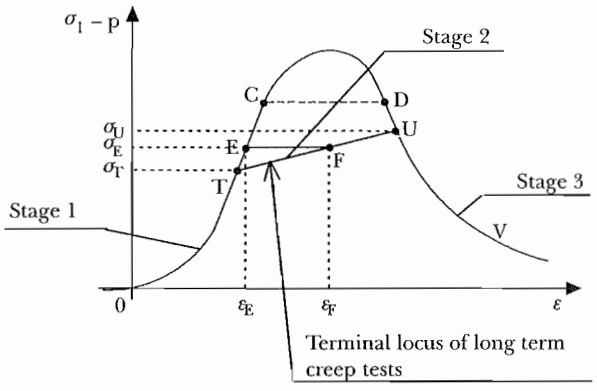

Fig. 1 – The complete stress-strain curve [LADANYI, 1993].
Fig. 1 – La curva sforzi-deformazioni completa [LADANYI, 1993].

term strength. The higher the applied stress and closer to the peak value, the shorter is the time to creep failure.

3. Proposed approach

As shown above, for stress values smaller than σ_T, which are held constant for a given time interval, the deformation behaviour does not exhibit any time-dependence. If a test is performed by increasing the applied stress up to σ_E, the following type of behaviour will be shown on the stress-strain curve (figure 1):

- the portion OE;
- the portion EF, where strain increases of (ε_F-ε_E) as the applied stress is held constant versus time.

The strain attained is equal to ε_F, greater than ε_E, and the terminal value of strain is reached without resulting into creep failure.

If the applied stress is greater than σ_U, the OCD curve will be followed and the long term conditions will be reached for a stress applied which is smaller than the peak value (tertiary creep stage). Under such a condition, if loading is continued, then the descending part of the curve DU will be followed.

The main idea which is proposed in order to describe the rock deformational response associated with squeezing behaviour is based on the above concepts. The purpose is to follow the "traditional" stress-strain curve up to a stress value representing the creep threshold, where the accumulated strain will increase progressively.

It is recognised that the rock behaviour around a tunnel is significantly more complex than observed in a laboratory test: the stress induced by excavation around a tunnel is related to a number of complex factors, which may change versus time, independent of the rock mass rheological behaviour (excavation sequences, delayed installation of lining, etc.). It is therefore questionable to analyse the squeezing behaviour on the basis of the onset of stress conditions which remain unchanged as delayed deformations occur (as is the case for the curve OEF): it is rather assumed that the stress-strain curve is of the OTUV type, according to the following three stages:

- stage 1. – elastic behaviour;
- stage 2. – viscous behaviour, which is partly not recoverable;
- stage 3. – when large deformations occur, which are predominantly not recoverable.

The implementation of a numerical model describing stage 1. does not represent anything new with respect to the use of constitutive laws applied in linearly and non linearly elastic conditions, as available in most computer codes.

However, stage 2. and 3. are to be considered part of the proposed approach: the implementation need to be carried out in order to be able to simulate both the large deformations and yielding behaviour which occur in squeezing conditions. With the objective in mind to adopt a technique which is easily applicable in practice, the theoretical equations describing such a behaviour have been based on plasticity theory. The mechanical parameters needed in such cases have been introduced, without resorting to the use of viscous parameters representing time-dependence, which are generally difficult to be directly assessed.

Each stage is characterised by a different model of behaviour (elastic the first one, plastic with parameters properly chosen the second and third one), so that the overall response with large deformations around a tunnel as a result of rheological behaviour can be described without introducing the time factor explicitly. It is important to underline that, from the point of view of constitutive modelling, the law which is proposed is not rigorous; however, a number of advantages are available which make it interesting for engineering applications

3.1. Analytical procedure

A description of the analytical procedure implemented in order to reproduce the trend of behaviour shown in Fig. 1, will be given in the following. To this end, the FLAC computer code [ITASCA, 1996] has been adopted as it enables the user to incorporate the desired changes in the constitutive laws and to define continuous functions of the strength parameters based on the attained stress-strain level. As anticipated, the available Mohr-Coulomb plasticity model has been adopted to suit the specific needs described above.

With the main purpose to describe the model adopted, reference is made for simplicity to uniaxial conditions (the transition to plane strain conditions is easily carried out in terms of tensors and invariants of the state of stress and strain). As shown in Fig. 2, the desired stress-strain law comprises a first stage (OA) in elastic conditions, a second stage (AB) of the plastic hardening type, and a third stage (below point B) of the plastic softening type.

With the FLAC code, the hardening/softening behaviour can be simulated with appropriate variations of the strength parameters (cohesion, friction and dilatation angles) as a function of plastic shear strain. The desired law of variation has been implemented by the powerful built-in programming language, FISH, which is incorporated in FLAC.

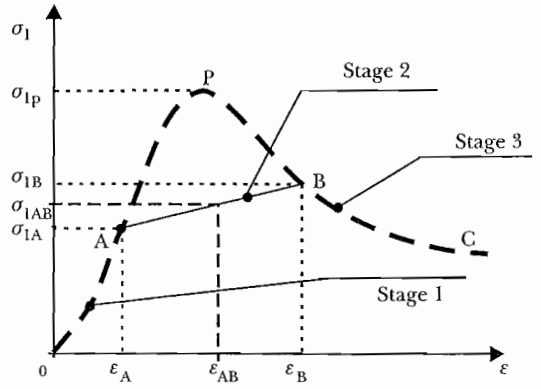

Fig. 2 – Proposed model for analysis of squeezing behaviour.
Fig. 2 – Modello di comportamento per lo studio del comportamento spingente.

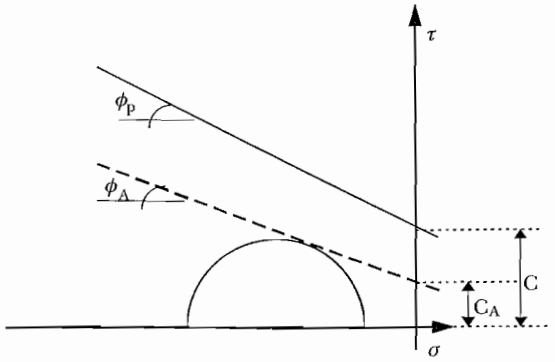

Fig. 3 – Mohr-Coulomb envelopes used to define transition from stage 1 to stage 2 on the complete stress-strain curve.
Fig. 3 – Inviluppi di Mohr-Coulomb adottati per definire la transizione dalla fase 1 alla fase 2 nella curva sforzi-deformazioni completa.

3.2. Linearly elastic stage

The first stage of the stress-strain curve is chosen to be linearly elastic, with the following stress-strain law in uniaxial conditions:

$$\sigma_1 = E\,\varepsilon_1 \tag{1}$$

The transition from stage 1. to stage 2. occurs at stress level σ_{1A}, when the material exhibits viscous partly irrecoverable strains. The σ_{1A} stress value can be chosen in practical applications and design analyses on the basis of experimental evidence and performance monitoring of real structures which allow one to assess the sensitivity to time-dependence; available data show that this stress level is always greater than 50% of the peak strength σ_{1p}.

The σ_{1A} stress value is attained by imposing a decrease of the peak strength parameters, so as to allow for a "contraction" of the yield surface and for the onset of irrecoverable strains of the creep type, prior to reaching the true yield stress conditions (Fig. 3). The expressions used in order to simulate the decrease in the strength parameters are as follows:

$$c_A = c_p \cdot \left(\frac{\sigma_1^A}{\sigma_1^p}\right)^2 \tag{2}$$

$$\phi_A = \frac{\sigma_1^A}{\sigma_1^p} \cdot \phi_p \tag{3}$$

3.3. Hardening stage

The hardening stage is simulated by introducing a plastic behaviour with hardening and the Mohr Coulomb criterion:

$$\sigma_1 = N_{\phi_{AB}} \cdot \sigma_3 + 2c_A \cdot \sqrt{N_{\phi AB}} \tag{4}$$

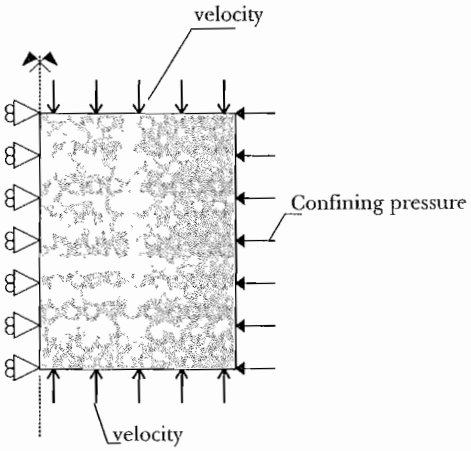

Figure 4 – Boundary conditions adopted for modelling the triaxial compression test.
Fig. 4 – Condizioni di vincolo per la simulazione della prova di compressione triassiale.

with $N_{\phi_{AB}} = \dfrac{1+sin\phi_{AB}}{1-sin\phi_{AB}}$

where the friction angle ϕ_{AB} is updated within the iterative procedure as a function of the plastic accumulated strain (ε_{AB} - ε_A) and of the state of stress (σ_{1AB}):

$$\phi_{AB} = \phi_A + \frac{\frac{1}{2}log(1+\varepsilon_{AB}-\varepsilon_A)}{1+200\cdot(\varepsilon_{AB}-\varepsilon_A)} \cdot \frac{\sigma_{1AB}}{\sigma_{1A}} \tag{5}$$

The cohesion is held equal to the value given by (2). The law of variation for the friction angle is chosen by trial and error, with the purpose to obtain a formulation which gives a linear trend for the AB portion of the stress-strain curve. The procedure adopted has been validated by numerical simulation of the stress-strain curves derived from triaxial compression tests, as shown in the following.

Eq. 5 simulates an approximately linear hardening law, characterised by a given slope. However, the use of the proposed approach in the analysis of other case studies could lead to appropriate changes, in order to improve the correspondence between the results of numerical modelling and performance monitoring. Therefore, the intention here is not to emphasise the use of (5), but rather the influence in terms of simulation of accumulated strains.

The form and iterative structure of Eq. 5 have been chosen for appropriate implementation of the proposed approach in the FLAC code. However, if other computer codes are used, the same law could be utilised with difficulty and fail in the simulation, as intended in the present paper, of the squeezing behaviour. In such a case, a similar expression need to be implemented, based on the same parameters, however to be validated with reference to numerical modelling of laboratory tests.

3.4. Long-term stage

The transition from stage 2. to 3. takes place for a plastic strain level which is a function of the current state of stress. The behaviour in the long term stage is again plastic according to the Mohr-Coulomb plasticity model, by using a softening formulation where the friction angle and cohesion decrease as a function of the plastic accumulated strain, up to attaining the residual values:

$$\phi_{BC}=13.4\cdot(\varepsilon_{BC}-\varepsilon_A)^{-0.2065} \quad (6)$$

$$c_{BC}=c_A\cdot\left(1-(\varepsilon_{BC}-\varepsilon_A)\right) \quad (7)$$

Also in this case the formulations have been implemented by using an empirical procedure, always with reference to stress-strain curves reproduced numerically. As far as the form of equations (6) e (7), the same observations made above hold true.

4. Implementation of the analytical procedure in the FLAC code

The implementation of the constitutive law described above has been effected by using two subprograms, the first one simulating the desired constitutive law, the second one in order to update the strength parameters.

4.1. Constitutive law

FLAC enables the user to define a constitutive law, different from those available in the code itself, by using special subprograms written with the programming language FISH. The procedure consists in the computation of the stress components starting with the current state of stress and accounting for stress increments according to given laws of behaviour, and repeating the procedure in sequence for all the elements in the model.

The subprogram which has been written in order to simulate the squeezing behaviour is based on the same procedure used for the Mohr-Coulomb model available in the FLAC code. Special functions have been implemented in order to compute:

- the accumulated plastic shear strain;
- the accumulated plastic tensile strain.

4.2. Strength parameters update

For the elements in the model where the current state of stress is such as to overcome the creep threshold value (given by the point A in Fig. 2), the friction angle is updated as a function of the strain (ε_{AB} - ε_A) and of the current state of stress according to Eq. 5. When the accumulated strain attains a given value, function of the applied state of stress, the material behaviour changes from stage 2. to 3., and the law of variation of the strength parameters changes accordingly with the updating by means of (6) and (7); it is noted that in this stage, previously called "long-term" stage, also the value of cohesion need to be changed.

The computational steps performed in order to update the strength parameters are carried out following the evaluation of the new state of stress and strain computed by means of the subprogram regarding the constitutive law; the updating is undertaken for all the elements which are in either stage 2 or 3. For simplicity, this subprogram is not used in each iterative step, but once n steps have been performed in sequence.

5. Model validation

With the purpose to validate the model and the procedure adopted, two simple cases have been considered: a triaxial compression test and the stress-strain distribution around a circular tunnel. The results obtained show a reasonable agreement between the stress-strain response obtained with the proposed model and the expected influence due to the material rheological behaviour.

5.1. Triaxial compression tests

Expressions (2), (3), (5), (6) e (7) have been derived by numerical simulation of a number of tests carried out under strain controlled conditions on a marly limestone. The physical property (γ), the de-

Tab. I – Properties of marl.
Tab. I – Proprietà della roccia in esame.

unit weight	$\gamma = 24$ kN/m^3
modulus of elasticity	E = 2 GPa
Poisson's ratio	$\nu = 0.3$
peak friction angle	$\phi_p = 30°$
residual friction angle	$\phi_r = 20°$
peak cohesion	$c_p = 0.48$ MPa
residual cohesion	$c_r = 0.01$ MPa

formability (E, ν), and strength characteristics (c_p, ϕ_p, c_r, ϕ_r) are shown in Tab. I.

The triaxial compression tests have been simulated numerically by using the FLAC code and a grid comprising 50 elements, with displacement velocity components imposed at the grid points on the lower and upper surface of the specimen. These values of velocity simulate a boundary displacement which is imposed on the specimen.

In order to minimise the inertial effects on the model response, the values of the velocity components are changed during each iteration as a function of the unbalanced force (maximum force at a grid point in the model): they are decreased if the unbalanced force is becoming too large, viceversa they are increased if this same force becomes too small. The velocity is not to be greater than a given maximum value.

A number of numerical analyses have been carried out with the purpose to simulate the following laws of behaviour:
- elasto-plastic with softening;
- "squeezing", for two different assumptions on the onset of time dependence:

$$\sigma_A = 0.5\ \sigma_p$$

$$\sigma_A = 0.75\ \sigma_p$$

Fig. 5 shows the deviatoric stress sigmav - axial strain *ev* plot obtained by a numerical simulation of the softening behaviour (continuous line) and of the squeezing behaviour (dashed line) for $\sigma_A = 0.5\ \sigma_p$ and three different values of the confining pressure: 1 MPa, 2MPa e 5 MPa. The comparison is quite interesting in order to assess the significance and potential of the proposed model for a phenomenological description of the time-dependent behaviour.

The validation of expressions (2) and (3) is possible based on the computation of the σ_A/σ_p ratio directly from the analyses performed: i.e., for a confining pressure equal to 5 MPa, the softening behaviour gives σ_p equal to 16.6 MPa; for the proposed model of behaviour, the stress-strain curve departs

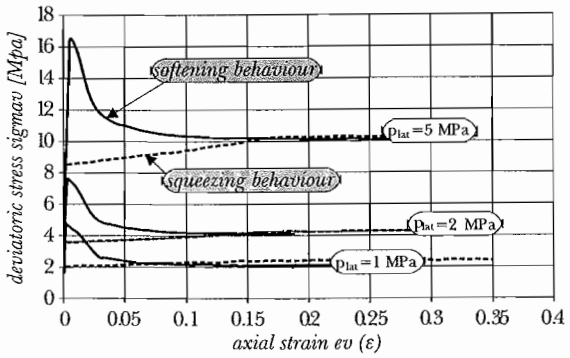

Fig. 5 – Stress-strain curves for softening and squeezing behaviour ($\sigma_A/\sigma_p = 0.5$). p_{lat} = lateral pressure.
Fig. 5 – Curve sforzo-deformazione nel caso di comportamento rammollente e di comportamento spingente ($\sigma_A/\sigma_p = 0.5$). p_{lat} = pressione laterale.

from the softening curve for a stress equal to 8.34MPa, corresponding to the σ_A value which is effectively the half of the peak value ($\sigma_A = 0.5\ \sigma_p$).

The slope of the line representing the terminal locus of a long-term creep behaviour is determined by equation (5), which is used to describe the variation of ϕ as a function of the accumulated plastic shear strain; in the analyses performed so far, the choice of the same slope has been effected independent of the results of creep tests, which were not available.

5.2. Solution for a deep circular tunnel

The proposed model has been as well validated by considering the solution for a deep tunnel of circular cross section in a homogeneous and isotropic stress field. The following analyses have been performed:
- softening behaviour;
- squeezing behaviour, with $\sigma_A/\sigma_p = 0.50$;
- squeezing behaviour, with $\sigma_A/\sigma_p = 0.75$.

The same strength and deformability properties have been utilised as shown in Tab. I, previously adopted for the simulation of the triaxial compression tests. The value of the in situ isotropic stress has been assumed equal to 1 MPa.

The comparison for the results obtained in the different calculations has been carried out with reference to: (i) tunnel convergence; (ii) plastic zone around the tunnel; (iii) stress distribution around the tunnel. The accuracy in the evaluation of the plastic zone is obviously dependent of the grid size, given that plasticity indicators are constant in each element.

Tab. II gives the radial displacement of the tunnel contour and the radius of the plastic zone for the analyses carried out. As expected, the values of both the radius of the plastic zone and the tunnel conver-

Tab. II – Values of plastic radius and convergence obtained by numerical modelling of different rock behaviour.
Tab. II – Valori di raggio plastico e di convergenza ottenuti dalle analisi numeriche per diversi tipi di comportamento.

modelling type	plastic radius [m]	convergence [mm]
proposed model (σ_A/σ_p = 0.50)	18.8	32.88
proposed model (σ_A/σ_p = 0.75)	7.03	5.03
softening model	5.40	3.57

gence are greater as the rock mass is more influenced by time-dependence, which is imposed by the σ_A/σ_p ratio.

Also to be noted is the distribution of both the radial and tangential stress around the tunnel shown in Figs. 6 and 7. The maximum value of the tangential stress computed for the squeezing behaviour, which is located at the boundary between the elastic and the plastic zone, is significantly smaller than that computed for the softening case. As described for the simulation of the triaxial tests, the numerical model is likely to reproduce the rock expected trend of behaviour, which is dependent from the level of accumulated strain, i.e. a decrease of the mechanical properties which determines a reduced load bearing capacity.

If consideration is also given to the extent of the plastic zone around the tunnel, it is possible to notice that the value of the plastic radius obtained in the case of squeezing behaviour is larger than the one computed assuming a softening behaviour (Fig. 8).

The same calculations (respectively for the softening behaviour and the squeezing behaviour when σ_A/σ_p = 0.50 and σ_A/σ_p = 0.75) have been carried out by introducing the presence of a concrete liner with thickness 20 cm, elastic modulus E_c = 200 GPa and Poisson's ratio ν_c=0.3, which is installed following a stress relief equal to 50% of the initial state of stress.

The results obtained are summarised in Tab. III: the values of tunnel convergence and extent of the plastic zone are found to be smaller than those obtained for the unlined tunnel. This is again of interest with respect to the ability of the proposed

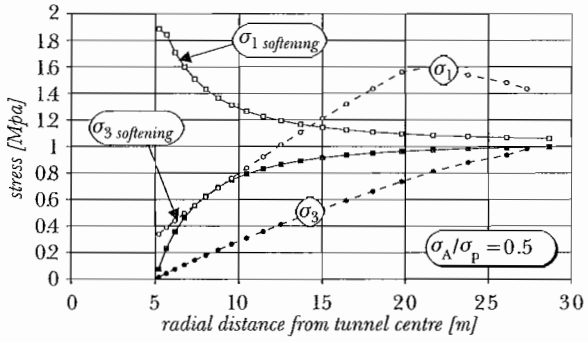

Fig. 6 – Radial and tangential stresses versus radial distance from tunnel centre. Comparison of solutions for strain-softening model and proposed model (σ_A/σ_p = 0.50) for p_0 = 1MPa.
Fig. 6 – Andamento delle tensioni radiali e tangenziali in direzione radiale a partire dal bordo della galleria. Confronto fra modello con ramollimento e modello proposto (σ_A/σ_p = 0.50) per p_0 = 1MPa.

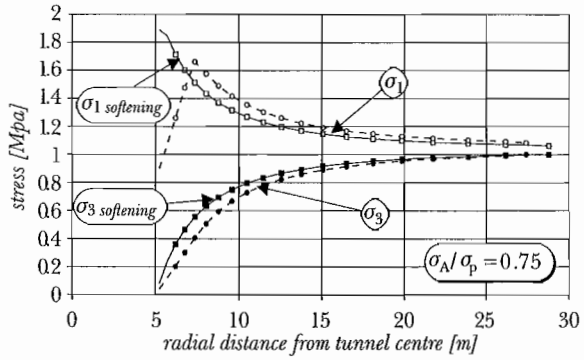

Fig. 7 – Radial and tangential stresses versus radial distance from tunnel centre. Comparison of solutions for strain-softening model and proposed model (σ_A/σ_p = 0.75) for p_0 = 1MPa.
Fig. 7 – Andamento delle tensioni radiali e tangenziali in direzione radiale a partire dal bordo della galleria. Confronto fra modello con ramollimento e modello proposto (σ_A/σ_p = 0.75) per p_0 = 1MPa.

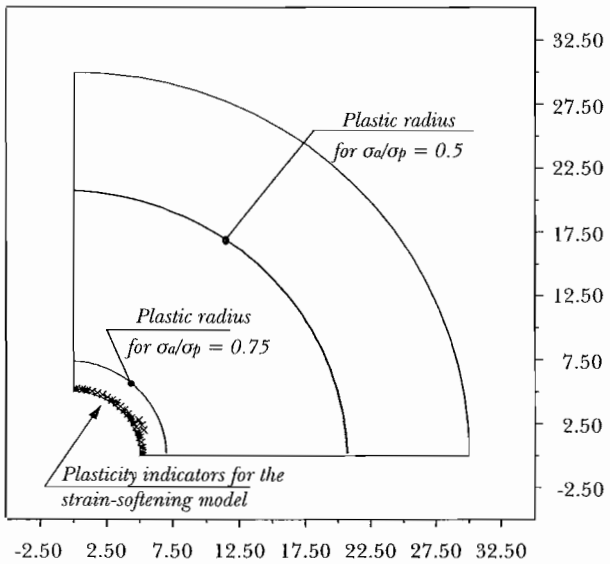

Fig. 8 – Plastic radii around the unlined tunnel. Comparison of solutions for strain-softening model and proposed model.
Fig. 8 – Zona plasticizzata intorno alla galleria in condizioni intrinseche. Confronto fra modello con rammollimento e modello proposto.

Tab. III - Values of plastic radius and convergence obtained by numerical modelling of different rock behaviour under the assumption of a confining pressure.
Tab. III – Valori di raggio plastico e di convergenza ottenuti dalle analisi numeriche per diversi tipi di comportamento e nell'ipotesi di presenza di una pressione di confinamento.

modelling type	plastic radius [m]	convergence [mm]
proposed model ($\sigma_M/\sigma_p = 0.50$)	11.6	16.27
proposed model ($\sigma_M/\sigma_p = 0.75$)	4.02	3.95
softening model	5.00	1.72

model to reproduce in a realistic way the behaviour of a tunnel under squeezing conditions.

Acknowledgements

The present study has been carried out with the financial support of the Minister of the University and Scientific Research within the National Project "Tunnelling in difficult conditions", coordinated by Prof. G. Barla in the Structural and Geotechnical Engineering Department of Politecnico di Torino (project n. 9708328160/1998).

Thanks are also due to Prof. S.C. Bandis and Dr. J.C. Sharp for their suggestions about the numerical implementation of the approach described in this paper.

References

BARLA G. (1995) – *Squeezing rocks in tunnels*. ISRM News Journal, vol. II, nn. 3-4, pp. 44-49.

LADANYI B. (1993) – *Time-dependent response of rock around tunnels*. Comprehensive Rock Engineering, Pergamon Press, vol. II, pp. 78-112.

ITASCA Consulting Group (1996) – *FLAC - Fast Lagrangian Analysis of Continua*. Ver. 3.3, User's Manual, voll. I-IV.

Modellazione numerica del comportamento spingente in galleria

Sommario

La nota descrive un procedimento numerico di modellazione, recentemente messo a punto, che prevede l'uso del Metodo delle Differenze Finite e del codice di calcolo FLAC. La legge sforzo-deformazione considerata simula tre diverse modalità di comportamento: la fase elastica, fino alla comparsa di deformazioni dipendenti dal tempo; la fase incrudente, che intende rappresentare il luogo dei punti in cui si esauriscono queste stesse deformazioni; la fase di comportamento rammollente. Sono presentati i risultati di alcune analisi numeriche, svolte allo scopo di simulare tipiche curve sforzo-deformazione in prove triassiali e di calcolare lo stato tensio-deformativo indotto nell'intorno di una galleria circolare profonda.